On the non-integrability of a family of Duffing-van der Pol oscillators

1993 J. Phys. A: Math. Gen. 26 6927

(http://iopscience.iop.org/0305-4470/26/23/033)

J. Phys. A: Math. Gen. 26 (1993) 6927–6942. Printed in the UK

On the non-integrability of a family of Duffing–van der Pol oscillators

T C Bountis†, L B Drossos†, M Lakshmanan‡ and S Parthasarathy‡

† Department of Mathematics, University of Patras, Patras, 26110 Greece

‡ Center for Nonlinear Dynamics, Department of Physics, Bharathidasan University, Tiruchirapalli 620024, India

Received 26 April 1993

Abstract. We investigate the non-integrability of a family of Duffing–van der Pol oscillators

$$\ddot{x}+\alpha\dot{x}(x^2-1)+x+\beta x^3=\gamma\cos\omega t \qquad (*)$$

by studying the analytic properties of the dynamics in complex time. We find that the solutions of (*) have no worse than *algebraic* singularities at t_*, with only $(t-t_*)^{1/2}$ terms present in their series expansions, unlike, for example, the $\alpha=0$ Duffing case, where, typically, $\log(t-t_*)$ terms arise. Still, when integrating (*) around long enough contours, a remarkably intricate pattern of square root singularities emerges, on different sheets, which appears to *prevent* solutions from ever returning to the original sheet. Such evidence of infinitely-sheeted solutions, termed the ISS property, has also been observed in a number of Hamiltonian systems and is illustrated here on a simple example of a single, first-order differential equation. We suggest that the ISS property is a necessary condition for *non-integrability*, i.e. *non-existence* of a complete set of analytic, single-valued constants of the motion, which would permit the complete integration of a dynamical system in terms of quadratures.

1. Introduction

It has been known for some time, mainly due to rigorous results by Ziglin and Yoshida [1–5], that the *non-integrability* (i.e. the non-existence of a complete set of analytic single-valued integrals) of many dynamical systems is connected with the fact that their solutions are, in general, *infinitely sheeted* functions of time in the complex domain. Typically, such solutions are seen to contain $\log(t-t_*)$ or $(t-t_*)^{\lambda}$ terms with λ irrational or complex, in their series expansions about a movable singularity, $t=t_*$, in the complex (time) t-plane [6, 7].

On the other hand, there also exist many examples of physically interesting systems, whose solutions have no worse than *algebraic* singularities in the complex domain. Some of these systems turn out to satisfy the so-called Weak-Painlevé property [8] and hence are completely integrable, in which case one might try to transform them to systems which are fully Painlevé, by some non-trivial change of coordinates [9, 10]. What happens, however, in the case of systems with only algebraic singularities, for which no such transformation can be found? How does one study their (non)integrability and its connection with the analytic structure of the solutions in complex time?

One answer to this question was recently proposed for a class of Hamiltonian systems of two degrees of freedom, whose solutions have only square root singularities

0305-4470/93/236927+16$07.50

in $t \in \mathbb{C}$ [11, 12]. It was found that, when one integrates numerically the equations of motion around long enough contours, an extremely complicated pattern of singularities emerges on different sheets, whose intricate branching apparently prevents the solutions from ever returning to their starting values on the original sheet. This suggests the existence of infinitely sheeted solutions, which we have called the ISS property and have conjectured it to be a necessary condition for non-integrability and chaotic behaviour in real time [5, 8, 11, 12].

In this paper, we present evidence that another physically interesting dynamical system, with only algebraic singularities, possesses the ISS property and is, therefore, strongly suspected to be non-integrable. This is a family of Duffing–van der Pol (DVP) oscillators described by the equation

$$\ddot{x} + \alpha\dot{x}(x^2 - 1) + x + \beta x^3 = \gamma \cos \omega t \tag{1.1}$$

where $\dot{x} = dx/dt$ and α, β, γ are constant parameters. Equation (1.1) may be considered as a model describing the propagation of voltage pulses along a neuronal axon, and has received a lot of attention recently by many researchers [13–16]. It is seen to exhibit a rich variety of bifurcations and chaotic phenomena in real time. Here we are interested *in the more mathematical question of the behaviour of the solutions of* (1.1) *in complex time.*

We would like, to stress, however that, besides being of mathematical interest, our exploration of the solutions of a dynamical system in complex time, offers also a practical test for non-integrability in two important cases:

(i) If a system *looks* integrable in real-time numerical experiments; and

(ii) if a system is *multi-dimensional* and integrability cannot be easily decided, e.g. by projections of orbits on spaces of lower dimensions.

Furthermore, as has been shown for several examples of periodically driven systems, it is interesting to study the *density* of singularities in the t-plane, which is seen to increase as a driving parameter is increased and the motion in real time becomes more chaotic [5, 7, 17, 18].

In section 2, we demonstrate first that the singularities of equation (1.1), for $\alpha \neq 0$, are all of square root type, i.e. the solution of (1.1), near these singularities, $t = t_*$, is of the form

$$x(t) = \tau^{-1/2} \sum_{n=0}^{\infty} a_n \tau^{n/2} \qquad \tau = t - t_* \tag{1.2}$$

with *no* $\log \tau$ terms arising (at the order where the second free constant enters) for *all* values of β and γ. We then investigate the analytic properties of the classical van der Pol equation (1.1) with $\beta = \gamma = 0$. What we find, at first, when integrating the equation around a contour enclosing only one pair of singularities of the original sheet, is that new singularities appear on other sheets, whose branching allows the solution to return to its initial value after a number of turns, which depends on the number of singularities enclosed in the contour.

If the contour is relatively small, we thus obtain evidence of *exact* returns, as the solutions keep 'seeing' the same small number of singularities and eventually return to their initial values, within the accuracy of our calculations. However, as the *size of the contour increases*, a sharp transition occurs, when one more singularity pair is included in the contour. A remarkably intricate singularity pattern emerges then and the ISS property of the solutions is evident, as they fail to return to their original values even after more that 200 turns.

In section 3, we examine the cases $\beta \neq 0$ and $\gamma \neq 0$ separately. For $\beta \neq 0$ and $\gamma = 0$ we find, again, around one singularity pair, clear evidence of ISS as follows: For reasonably small contours, the *projections* of singularities on the same sheet form clusters with complicated structure and the absolute difference of the solution from its value on the original sheet grows *linearly*, on the average, at least over the first 200 turns. However, for somewhat larger contours, a sharp transition occurs again to a complicated, cloud-like singularity pattern, with the solutions differing significantly and chaotically from their starting values.

Similar ISS phenomena are observed in the case $\gamma \neq 0$ and $\beta = 0$ ($\alpha \neq 0$). Here, however, there is an additional interesting complication: due to the presence of $\cos \omega t$ terms in the expansions of the solution around a singularity the radius of convergence of these series decreases exponentially in the $|\mathrm{Im}(t)|$ direction. This leads to a *clustering* of singularities on the *same* sheet, as has been observed in the past, in the analysis of other periodically driven oscillators [5, 7, 17, 18]. Furthermore, just as was found in those cases, here also, the singularity pattern appears to grow denser as the value of $\gamma > 0$ is increased and the motion becomes more chaotic in real time.

In section 4, we present, for pedagogical purposes, our analysis of the solutions of a simple-looking first order equation

$$\frac{\mathrm{d}x}{\mathrm{d}t} = x - x^3 + \varepsilon t + \delta \tag{1.3}$$

which has only square-root singularities in $t \in \mathbb{C}$, for all values of ε and δ. We find that all these solutions are finitely sheeted, for $\varepsilon = 0$, which demonstrates the integrability of (1.3), while in the non-integrable case $\varepsilon \neq 0$ infinite sheeted solutions are found, in a similar way, as described above.

Finally, section 5 contains a discussion of our results and some general remarks on the singularity analysis of dynamical systems in complex time.

2. Singularity analysis of the van der Pol equation

Let us begin our analysis of the family of DVP oscillators

$$\ddot{x} + \alpha \dot{x}(x^2 - 1) + x + \beta x^3 = \gamma \cos \omega t \tag{2.1}$$

by showing that, for $\alpha \neq 0$, all of its solutions possess only square-root singularities in the complex t-plane. We will then proceed to investigate in this section the pure van der Pol case: $\beta = \gamma = 0$.

As is usually done in singularity analysis [5–8], one starts by finding all possible leading behaviours of the solutions, near a (movable) singularity $t = t_*$. In the case of (2.1), there is only one such behaviour:

$$x(t) \sim \left(\frac{3}{2\alpha}\right)^{1/2} \tau^{-1/2} \qquad \tau = t - t_* \tag{2.2}$$

as $\tau \to 0$, for $\alpha \neq 0$. Proceeding to the determination of higher-order terms in

$$x(t) = \left(\frac{3}{2\alpha}\right)^{1/2} \tau^{-1/2} + a_1 + a_2 \tau^{1/2} + a_3 \tau + a_4 \tau^{3/2} + \ldots \tag{2.3}$$

one easily finds, upon equating in (2.1) terms of order τ^{-2}, $\tau^{-3/2}$, τ^{-1} respectively:

$$a_1=0 \qquad a_2=\left(\frac{3}{2\alpha}\right)^{1/2}\left(\frac{3\beta}{2\alpha}+\frac{\alpha}{2}\right) \qquad a_3=\text{arbitrary.} \tag{2.4}$$

This implies that the second free constant, a_3 (the first one is t_*) of the solution is compatible with a series expansion of the form (2.3) for all values of β and γ. Hence no logarithmic terms (or any other kind of singularities) arise and the general solution of (2.1) near $t=t_*$ can be written as

$$x(t)=\tau^{-1/2}\sum_{n=0}^{\infty} a_n\tau^{n/2} \qquad \tau=t-t_*. \tag{2.5}$$

Clearly the periodic forcing term in (2.1) gives

$$\gamma\cos\omega(\tau+t_*)=\gamma\cos\omega t_*\left(1-\frac{\omega^2\tau^2}{2}+\ldots\right)-\gamma\sin\omega t_*\left(\omega\tau-\frac{\omega^3\tau^3}{6}+\ldots\right) \tag{2.6}$$

and will start contributing in equation (2.1) at order τ^0, adding a $\gamma\cos\omega t_*$ to the equation from which the coefficient a_5 is calculated.

Furthermore, as we have shown in [19], one can prove, using Weierstrass majorant method, that the series (2.5) converges in the punctured disc:

$$D=\{\tau\neq 0, \quad \text{with } |\tau|<R<\infty\}$$

within a finite radius of convergence $R>0$, which, at least numerically, is seen to extend to the singularity nearest to t_* in the complex t-plane.

So the solutions of (2.1), for $\alpha\neq 0$, are *locally* (i.e. near every t_*) finitely branched and finitely sheeted. Does that mean that they are also globally finitely sheeted?

To find out let us integrate the equation of motion (2.1) numerically in the complex t-plane, along simple rectangular contours enclosing more than one singularity of the primary Riemann sheet. This is done using the ATOMFT 2.51 (1991) algorithm, which is a more recent version of the original ATOMCC program developed by Chang and Corliss [20, 5, 6]. All computations were carried out in double precision on a PC 386 taking less than a minute of execution time for each turn around a typical contour.

Let us set $\beta=\gamma=0$ and consider the pure van der Pol equation

$$\ddot{x}+\alpha\dot{x}(x^2-1)+x=0 \qquad \alpha>0. \tag{2.7}$$

As is well known, all solutions of this equation tend to a limit cycle in the $x, \dot{x}$ phase plane, whose amplitude is bounded between -2 and 2, while its velocity increases without bound as α increases to larger and larger values [21]. Equation (2.7) is non-integrable in the sense that it cannot be transformed to any of the 50 second-order equations discovered by Painlevé [5, 8], whose solutions are single-valued (except for a number of isolated poles) in the complex t-plane.

But in what sense are the solutions of (2.7) multivalued? Let us choose, for convenience, initial conditions $t=0$, which place our solution near the limit cycle, i.e.

$$x(0)=2.0 \qquad \dot{x}(0)=0 \tag{2.8}$$

and take α values of order unity, at which the period of the limit cycle oscillations is nearly 2π. Then the singularities of the solution, on the primary sheet, form a row of conjugate pairs placed along the Re t axis, at nearly π-distances between each pair, as shown in figure 1.

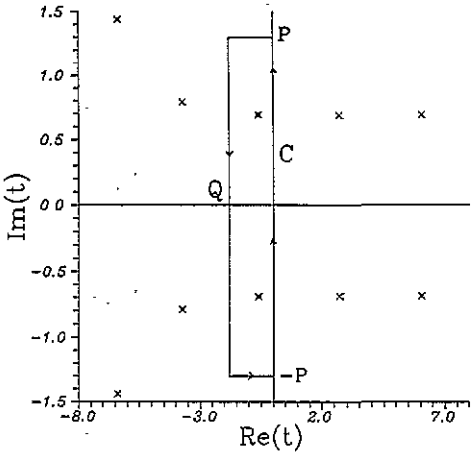

Figure 1. Arrangement of singularities on the primary Riemann sheet of the solutions of (2.7), with $\alpha = 1$ and initial conditions (2.8).

The reason for this arrangement is that the Fourier representation of the solution diverges in the $|\mathrm{Im}\ t|$ direction at all real t values where the amplitude of the oscillation is largest, i.e. at the maxima and minima of $x(t)$, $t \in \mathbb{R}$, which occur at near multiples of π. Now let us enclose the pair of singularities nearest to the Im t axis in a rectangular contour C (see figure 1), which intersects the Re t axis at $Q = -1.8$ and whose vertices on the Im t axis are located at the points P and $-P$.

We will now make several turns around C and compute the values of $x(t)$, $\dot{x}(t)$, at P, after the Nth turn: $x_P(N)$, $\dot{x}_P(N)$, respectively. In particular, we are interested in the values of

$$\Delta x_P(N) = |x_P(N) - x_P(0)| \qquad \Delta \dot{x}_P(N) = |\dot{x}_P(N) - \dot{x}_P(0)| \tag{2.9}$$

i.e. the absolute differences of x and $\dot{x}$ at P after N turns, from their values at the beginning of the first turn.

In table 1 we list these differences for several values of P between 1.1i and 1.3i. We find, for these contours, evidence of *finitely sheeted* solutions (FSS), returning to their starting values after a number of turns N, which equals the number of singularities

Table 1

P	N	Number of singularities in Contour C	$\Delta x_P(N)$	$\Delta \dot{x}_P(N)$
1.09i	7	6	7.8×10^{-14}	3.2×10^{-14}
1.18i	7	6	1.0×10^{-12}	5.7×10^{-13}
1.24i	7	6	7.0×10^{-13}	3.6×10^{-13}
1.25i	7	6	1.6×10^{-11}	1.6×10^{-11}
1.255i	9	8	1.9×10^{-8}	1.7×10^{-8}
1.27i	9	8	8.5×10^{-10}	6.5×10^{-10}
1.30i	9	8	2.7×10^{-9}	2.9×10^{-9}

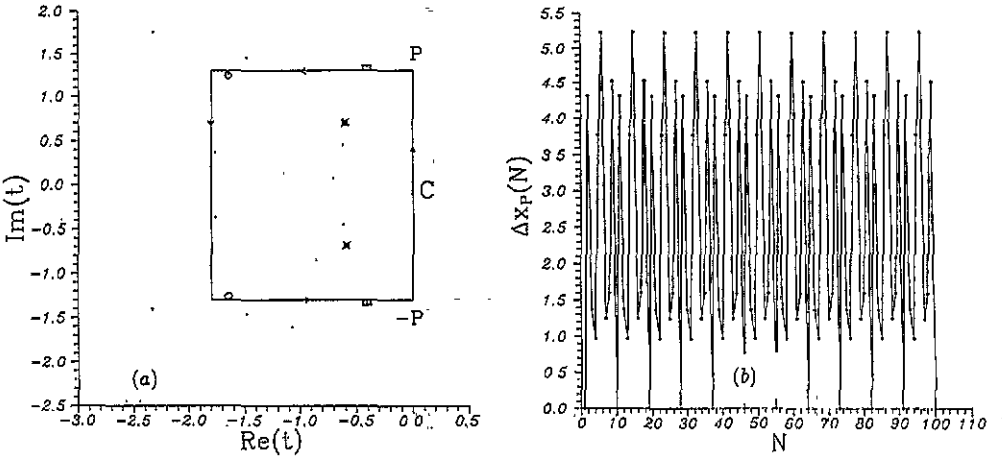

Figure 2. Complex time integration of (2.7), with $\alpha = 1$ and initial conditions (2.8) around two of the primary sheet singularities of figure 1 (marked by × here). (*a*) The upper right corner of contour is at $P = 1.3$i and no new singularities, other than the ones shown here, appear, even after 200 turns around C. (*b*) The solution differences $\Delta x_P(N)$, cf. (2.9), showing clear evidence of FSS as they return to 0, within 10^{-9}, after every nine turns.

enclosed in C, plus one. Note, in figure 2(*a*), for the $P = 1.3$i case, that these singularities belong to different sheets (the singularities of the primary sheet are marked by × in the figure).

Observe that the number of turns N, needed for the solutions to recover their original values at P, increases by 1 for $P > 1.2525$i, i.e. when the singularities marked by ⊙ have been included in C. In figure 2(*b*) we have plotted the values of $\Delta x_P(N)$ for several turns in the $P = 1.3$i case. Even though the differences of $\Delta x_P(N)$ from 0, after every nine turns, has increased from 10^{-12} to 10^{-9} (table 1), this is still considered as evidence of FSS, within the accuracy of our computations.

A dramatic change occurs in these pictures, however, when $P \geqslant 1.33194$i, which is the (positive) imaginary part of the singularity pair marked by ⊡ in figure 2(*a*). Compare figures 3(*a*), (*b*) and 4(*a*), (*b*) for $P = 1.33191$i and $P = 1.33197$i, respectively. In figures 3(*a*), (*b*) the singularity pattern and the $\Delta x_P(N)$'s are practically identical with the corresponding ones of figures 2(*a*), (*b*). However, in figures 4(*a*), (*b*), for $P = 1.33197$i, the situation is entirely different: a cloud of new singularities has emerged, whose branching does not allow the solution to return to its original value even after more than 200 turns.

This evidence of ISS persists for larger values of P, as well. The cloud of singularities remains equally dense and the chaotic oscillations of $\Delta x_P(N)$ are qualitatively similar in every case, differing only in their detailed structure. That these pictures are not caused by numerical errors in seen by the fact that when the calculations are repeated for slightly different Ps (e.g. $P = 1.332$i and $P = 1.333$i) *exactly the same* singularity pattern and $\Delta x_P(N)$ oscillations are observed, even after 200 turns.

There is, also, an interesting phenomenon of sensitivity of solutions to small changes in their initial conditions! When we took $P = 1.5$i and varied the initial conditions (2.8) to

$$x(0) = 2.000\,01 \qquad \dot{x}(0) = 0 \tag{2.10}$$

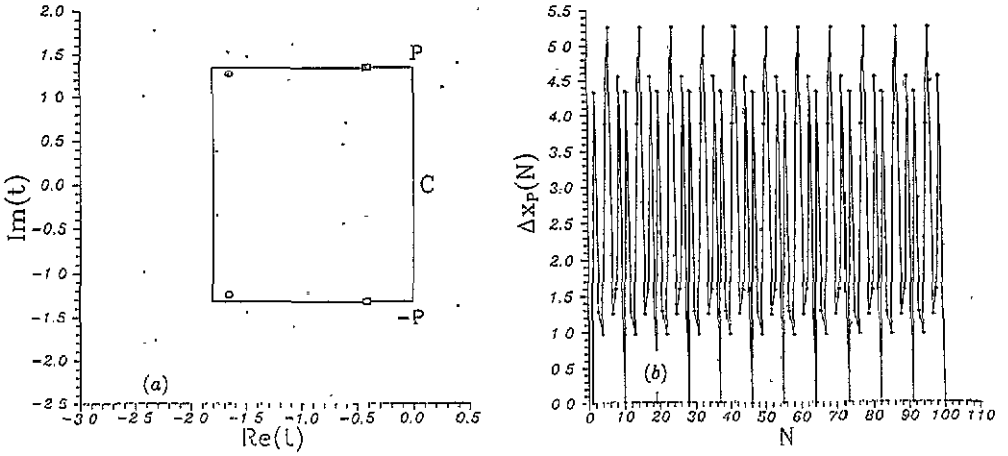

Figure 3. (*a*) Same as figure 2(*a*), with $P=1.33191$i, just before the singularity marked by ⊡ has been included in C. (*b*) Same as figure 2(*b*), at this P value. Note the similarity between these two figures.

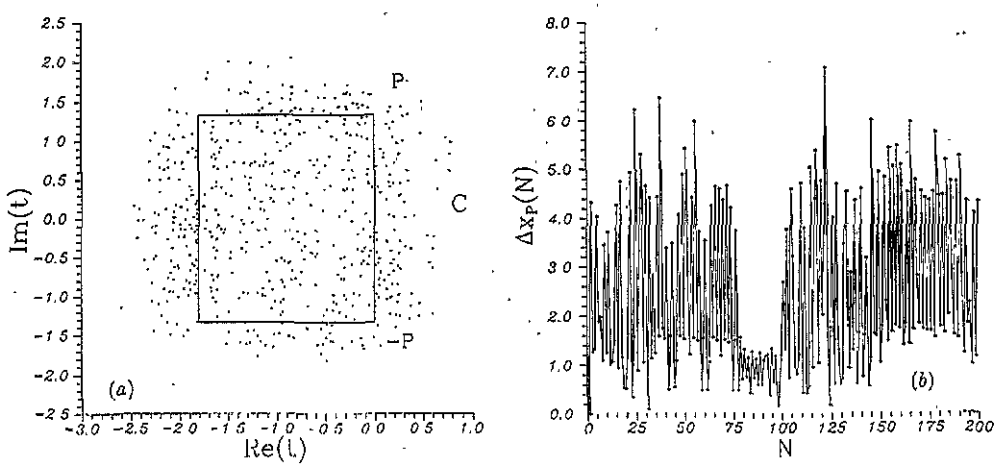

Figure 4. (*a*) Same as figures 2(*a*) and 3(*a*), with $P=1.33197$i, i.e. just after the singularity ⊡ has been included in *C*. An 'explosion' of singularities has occurred and the figures are now completely different. (*b*) New singularities of figure 4(*a*), now, prevent the solution from recovering its initial value, even after $N=200$ turns.

the $\Delta x_P(N)$ oscillations started to differ significantly from the (2.8) case, after the 65th turn. Thus, we can say that, even though (2.7) is, by definition, *not* chaotic in *real* time (since it only describes planar motion), it does exhibit chaotic behaviour in complex time, where its non-integrability becomes apparent via the ISS property.

3. DVP oscillators with $\beta\neq 0$ and $\gamma\neq 0$

We now turn to the investigation of the more general case of DVP oscillators (2.1) with $\beta\neq 0$ and $\gamma\neq 0$, separately. Before we start, however, we should point out, that the

condition $\alpha \neq 0$ is very crucial for the results of this paper. Indeed, if we set $\alpha = 0$, the singularities are of an entirely different type, determined by the βx^3 Duffing term of (2.1): Near these singularities, $x = (-2/\beta)^{1/2}\tau^{-1}$ and $\log \tau$ terms appear in the series expansions, with well known ISS properties, which were studied in detail in earlier publications [7, 22, 23].

For $\alpha \neq 0$, however, the Duffing and periodic terms in (2.1) do not alter the square-root nature of the singularities (2.2), about which the solutions are given by series expansions of the form (2.5), as was shown in the previous section.

Our main observation, in this section, is that the ISS property is also present for $\beta \neq 0$ and for $\gamma = 0$ in (2.1). To see this, let us consider first the unforced DVP oscillator, with $\gamma = 0$ in (2.1)

$$\ddot{x} + \alpha\dot{x}(x^2 - 1) + x + \beta x^3 = 0. \tag{3.1}$$

This equation also supports limit cycle oscillations, which for β of order unity, are numerically seen to be very similar to the ones of the van der Pol case ($\beta = 0$). We may, therefore, start out investigations, for small β, using the same kind of contour C, as in section 2, around one singularity pair of the primary sheet, and the same initial conditions: $x(0) = 2.0$, $\dot{x}(0) = 0.0$.

As we see in figure 5, for $\beta = 0.25$ and $\alpha = 1$, when we integrate around a contour C containing the two singularities marked by $S, \bar{S}$ in figure 5(a), new singularities appear on different sheets, which are grouped together in the form of clusters. In figure 5(b), we exhibit a magnification of one of these clusters, which shows a complicated (possibly fractal) structure. The result of this accumulation of singularities is shown in figure 5(c): The solutions around C show clear evidence of ISS, as their differences from their starting values at P, are of order 10^{-3}, after each turn, and grow linearly with N, at least up to $N = 200$.

We have checked that these results are not caused by numerical errors, as follows: Varying the vertical length of C, we obtain, for several $P \geqslant \mathrm{Im}(S)$ the same pictures as depicted in figure 5. On the other hand, if $P < \mathrm{Im}(S)$, there is no such singularity accumulation; only two singularities appear in C and the solutions return to their original values, after three turns, with an accuracy of order 10^{-11}.

Finally, by increasing further the vertical length of the contour (taking $P > \mathrm{Im}(S)$), we also find, here, a sudden transition to a 'scatter' of singularities, similar to the cloud-like patterns, observed in the van der Pol case, $\beta = \gamma = 0$.

Let us now consider the $\beta = 0$, $\gamma \neq 0$ case:

$$\ddot{x} + \alpha\dot{x}(x^2 - 1) + x = \gamma \cos \omega t. \tag{3.2}$$

We will take again $\alpha = 1$, the same initial conditions and the same contour C, as in section 2. Recall that with $P \leqslant 1.33\mathrm{i}$, we had obtained there (with $\gamma = 0$) evidence of FSS, as shown in figures 2 and 3. Identical pictures are obtained here also for small enough values of γ, e.g. $\gamma = 0.01$.

When γ is increased, new singularities enter in the contour and a sharp threshold exists, again, at which an explosion of singularities occurs within the boundaries of C and the differences $\Delta x_P(N)$ start to oscillate chaotically, yielding strong evidence of ISS. For the contour chosen here, with $P = 1.325\mathrm{i}$, this transition occurs at $\gamma \geqslant 0.015$.

When γ is increased further, e.g. to $\gamma = 0.2$, ISS phenomena are seen to persist and become even stronger, as the $\Delta x_P(N)$ differences oscillate further away from zero, than in the small γ case. However, when we increased γ to 0.5, FSS was observed! The reason for this is that, at this value of γ, the crucial singularity (which ushers in the singularity cloud and yields ISS) has passed outside the path of our contour. When the contour is

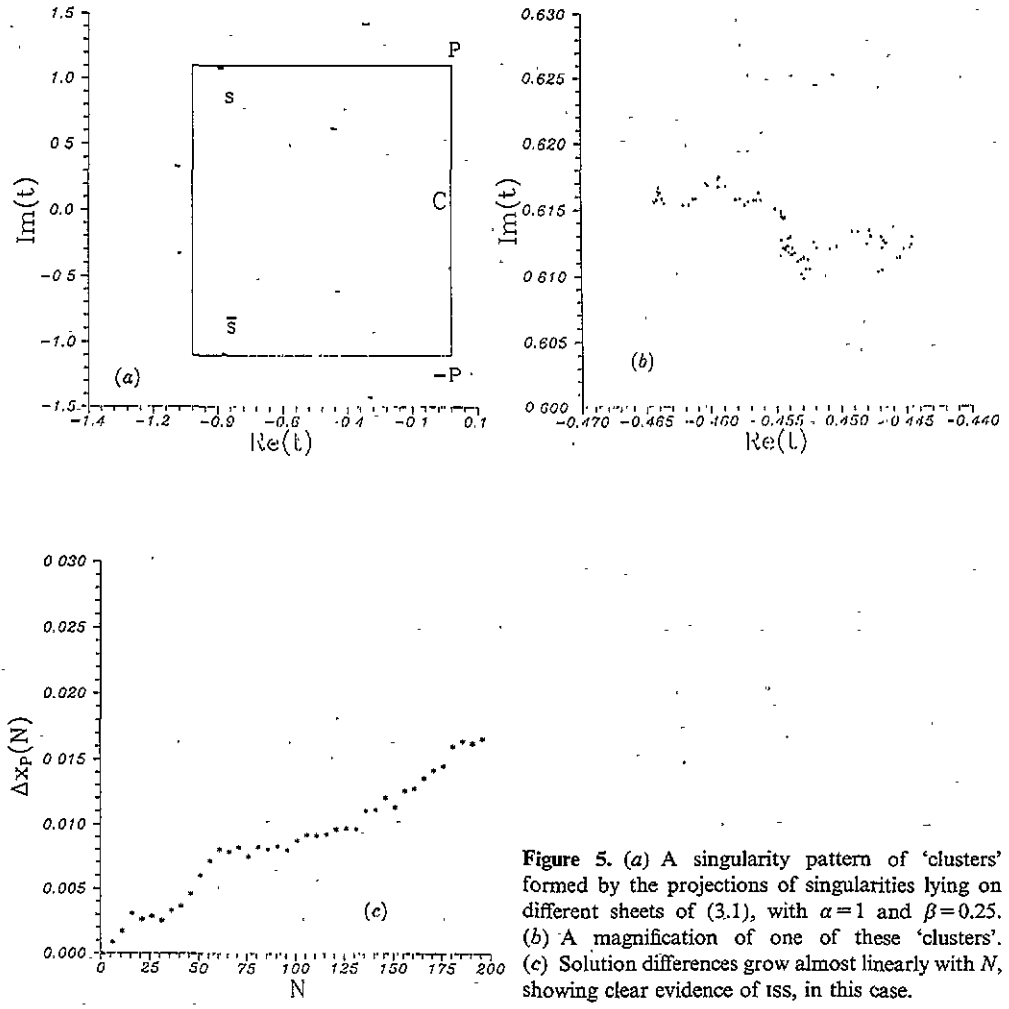

Figure 5. (*a*) A singularity pattern of 'clusters' formed by the projections of singularities lying on different sheets of (3.1), with $\alpha=1$ and $\beta=0.25$. (*b*) A magnification of one of these 'clusters'. (*c*) Solution differences grow almost linearly with N, showing clear evidence of ISS, in this case.

appropriately enlarged to contain that singularity, ISS is recovered at large values of γ, as before.

We end this section, with the observation and description of a different type of singularity *clustering*, in the complex t-plane in the $\gamma\neq 0$ case. As we have remarked elsewhere [11, 12], algebraic singularities are generally *not* expected to cluster on the same Riemann sheet. The basic reason for this is that, in the analysis of the solutions near a singularity, none of the clustering structures produced by τ^{λ} (λ complex or irrational) [6] or $\log\tau$ terms [22, 23] can occur with rational powers of τ. Indeed, none was observed, in all the autonomous systems with algebraic singularities considered so far [11, 12].

However, even though, by themselves, algebraic singularities do not cluster, in the presence of a periodic forcing term, like the one in (3.2), the following can happen: Terms of the form

$$\gamma\, e^{\pm i\omega t_*}=\gamma\, e^{\mp\omega t_I}(\cos\omega t_R \pm i\sin\omega t_R) \tag{3.3}$$

enter in the coefficients of the series (2.5), as explained in section 2, cf. (2.6), where $t_*=t_R+it_I$. This means that these terms will grow exponentially in the Im t direction,

due to the $\exp(\mp\omega t_I)$ factor in (3.3). Hence, in this direction, the radii of convergence of (2.5) are expected to decrease exponentially and singularities will therefore accumulate on the same sheet.

Such accumulation was indeed observed near primary sheet singularities of the DVP oscillator (2.1). Taking $\alpha=0.1$, $\beta=0.01$ and $\gamma=0.001$, we find near the Im t axis (and

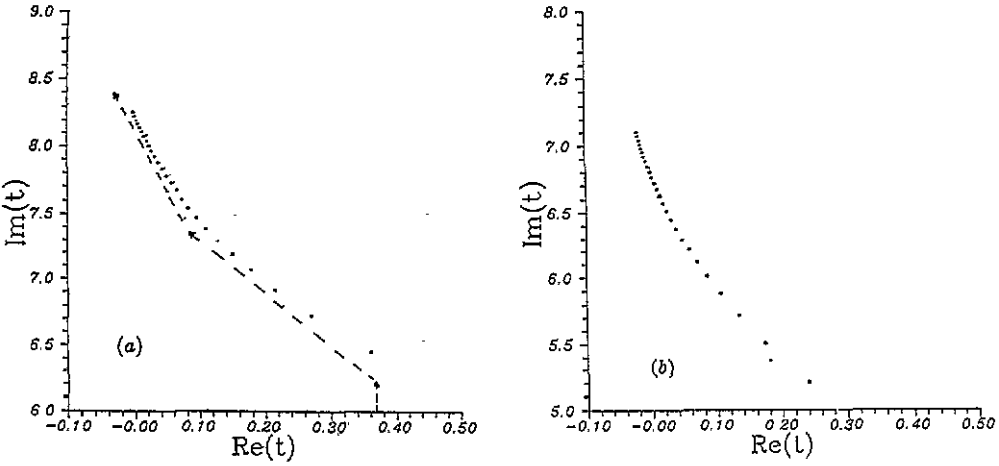

Figure 6. (*a*) Singularity accumulation in the Im $t>0$ direction for (2.1) with $\alpha=0.1$, $\beta=0.01$ and $\gamma=0.001$. (*b*) Note how the pattern of (*a*) 'condenses' when the value of γ is increased to $\gamma=0.01$. The dashed line indicates the integration path followed by ATOMFT to 'see' these singularities.

sufficiently far from the Re t axis) the picture shown in figure 6(*a*). To 'see' these singularities, we followed the path shown by the dashed line in the figure.

According to the argument given above, besides t_I, the value of the parameter γ should also affect the radii of convergence of the solution near every t_*, though not exponentially, of course, as in the case of t_I. To find out, we increased the value of γ ten times and performed the same experiment, looking at the same singularities in this region of the complex t-plane. The result, shown in figure 6(*b*), demonstrates clearly, on the same scale, that the relative distances between the singularities of figure 6(*a*) has decreased and the pattern has become denser.

It is in this sense that we speak of the real time motion of a dynamical system being reflected, in some way, by the analytic properties of the solutions in complex time.

4. A first-order equation and other examples

In this section, we illustrate some of the phenomena discussed in the previous sections on the first order differential equation

$$\frac{dx}{dt}=x-x^3+\varepsilon t+\delta. \tag{4.1}$$

Since a rigorous theory of the results presented in this paper is still lacking, our purpose here is to test the validity and implications of our analysis on the simplest, non-trivial example imaginable. Later in this section, we will consider a more 'realistic' model and

discuss the usefulness of our methods in distinguishing between integrability and non-integrability in Hamiltonian systems with only algebraic singularities.

Let us start by writing down the exact solution of equation (4.1), for $\varepsilon=\delta=0$

$$x_0(t)=[1+e^{2(t_0-t)}]^{-1/2} \tag{4.2}$$

with initial condition $x_0(0)\in(0,1)$. This expression, when expanded about one of its singularities,

$$t_*^{(k)}=t_0+(2k+1)\frac{i\pi}{2} \qquad k\in\mathbb{Z} \tag{4.3}$$

yields a power series in $\tau=t-t_*^{(k)}$, which involves only odd powers of $\tau^{1/2}$, i.e.

$$x_0(t)=[1-e^{-2\tau}]^{-1/2}=\tau^{-1/2}\sum_{n=0}^{\infty}c_n\tau^n \tag{4.4}$$

c_n being the appropriate Taylor coefficients. These are both locally and globally finitely sheeted (FSS), since they recover their initial values at some point P of a closed contour of arbitrary size, after one or two turns only, depending on whether an odd or even number of singularities (4.3) are enclosed in the contour.

What about the $\varepsilon=0$, $\delta\neq0$ case? Here the situation is slightly more complicated: equation (4.1) can be integrated by separation of variables, to yield

$$t-K=\int\frac{dx}{x-x^3+\delta}=\ln[(x-x_1)^A(x-x_2)^B(x-x_3)^C] \tag{4.5}$$

where

$$A=\frac{-1}{(x_2-x_1)(x_3-x_1)} \qquad B=\frac{-1}{(x_1-x_2)(x_3-x_2)} \qquad C=\frac{-1}{(x_1-x_3)(x_2-x_3)} \tag{4.5a}$$

K being an arbitrary constant and $x_1<x_2<x_3$ the roots of $x-x^3+\delta$. Unfortunately, equation (4.5) cannot be inverted, in general, to give an explicit expression of $x(t)$ as a function of t. Thus the complete sheet structure of the solutions of (4.1) cannot be analytically revealed, even in this simple case.

We can, however, obtain from (4.5) explicit information about the location of the singularities of $x(t)$ in the complex t-plane. Let us consider, for example, a value of δ for which x_1, x_2, x_3 (and hence also A, B and C) are real. Rewriting (4.5) in the form

$$e^{t-K}=(x-x_1)^A(x-x_2)^B(x-x_3)^C \tag{4.6}$$

and taking $|x|\to\infty$ near a singularity $t=t_*$, we find

$$e^{t_*-K}\sim|x|^{A+B+C}=1$$

since $A+B+C=0$, cf. (4.5a). Thus, singularities are located at

$$t_*^{(l)}=K+2il\pi \qquad l\in\mathbb{Z}. \tag{4.7}$$

Given now a real initial condition $x(0)=x_0$, with $x_1<x_2<x_0<x_3$, say, we obtain from (4.6)

$$K=K_m=M+\pi i(2m+1)C \qquad m\in\mathbb{Z} \tag{4.8}$$

where $\exp(-M)=(x_0-x_1)^A(x_0-x_2)^B(x_3-x_0)^C$. Combining now (4.7) and (4.8) we finally find a set of singularities

$$t_*^{(l,m)}=M+\pi i[(2m+1)C+2l] \tag{4.9}$$

which is, in general, dense on the line $t=M\in\mathbb{R}$.

However, these singularities belong to different sheets and only a finite number of them appears every time one integrates (4.1) (with $\varepsilon=0$) around a specific closed path. Taking, for example, $\delta=0.05$ and the rectangular contour shown in figure 7(*a*), which eventually encloses 18 such singularities, we find *exact returns* to the starting values at the point P, after $N=13$ turns, with initial condition $x(0)=1/\sqrt{2}$, see figure 7(*b*). Increasing δ to $\delta=0.1$ and keeping everything else the same, 24 singularities are seen to lie within the contour, and clear evidence of FSS is obtained after $N=19$. Observe that, in this example, the number of the enclosed singularities and the number of turns needed for exact return to the original sheet are not related in the same simple way, as in the van der Pol case of section 2 (table 1).

Thus (4.1) with $\varepsilon=0$ was found to have *finitely sheeted* solutions in every case, a result which is compatible with the fact that it is an integrable (if not explicitly solvable) equation, cf. (4.5). This equation has also been tested by the so-called poly-Painlevé criterion in [8], according to which, it may also be termed *integrable*, since it possesses a (non-dense) *lattice* of singularities in the complex x-plane.

What happens now if we let $\varepsilon\neq 0$? First of all, the solutions near a singularity, just as in the $\varepsilon=0$, $\delta\neq 0$ case, possess the series expansion

$$x(t)=\tau^{-1/2}\sum_{n=0}^{\infty} a_n\tau^{n/2} \qquad \tau=t-t_* \tag{4.10}$$

where all (even and odd) powers of $\tau^{1/2}$ enter in the sum. These singularities, however, do not lie on a straight line, as in the $\varepsilon=0$ case. They are found to have a much more complicated structure, which may be responsible for the ISS property of this case.

Using a contour similar to that of figure 7, containing three primary sheet singularities a rich pattern is revealed, with new singularities constantly appearing on a set of

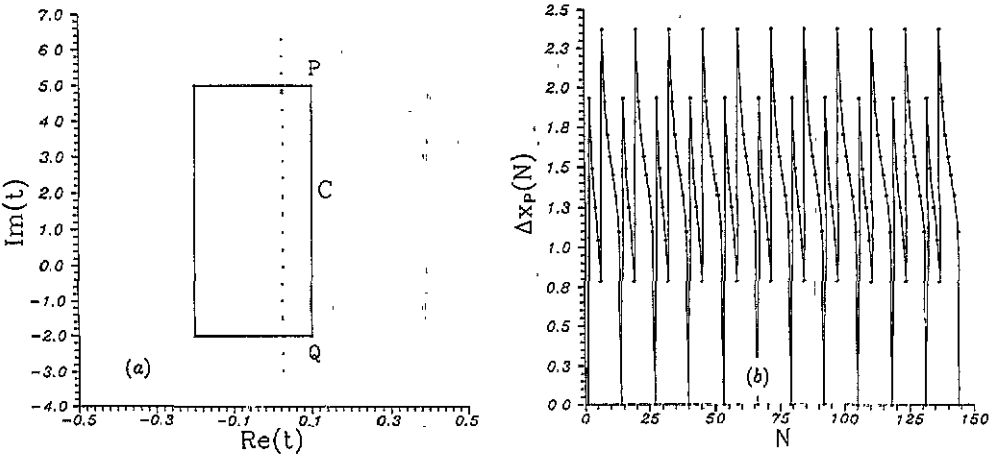

Figure 7. (*a*) Singularity patterns for (4.1) with $\varepsilon=0$ and $\delta=0.05$ and an asymmetric contour C with right corners at $P=5i$ and $Q=-2i$. (*b*) Evidence of FSS is found for (*a*), as the solutions are seen to return to their initial values after every 13 turns.

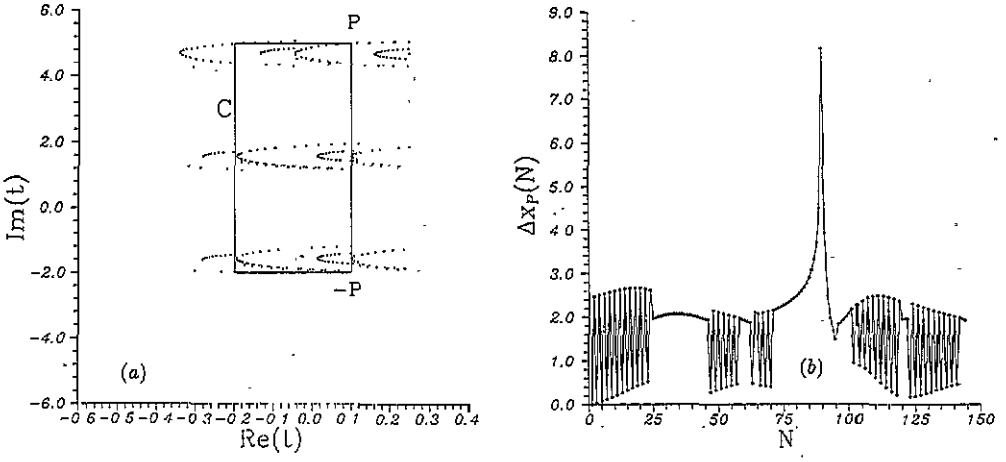

Figure 8. (*a*) Integration of (4.1) for $\varepsilon=0.01$, $\delta=0$, enclosing three singularities of the primary sheet. New singularities are seen to constantly appear yielding (*b*) ISS evidence, as the solutions fail to return to their starting values, even after 200 turns.

nested parabolic curves shown in figure 8(*a*). The solution $x(t)$, respectively, exhibits unpredictable oscillations of differences $\Delta x_P(N)$ from its starting value at P, showing clear signs of being infinitely sheeted, see figure 8(*b*).

Finally, we mention here one example of a Hamiltonian system

$$H=\tfrac{1}{2}\dot{x}^2+\tfrac{1}{2}x^2(1+\varepsilon_1\cos\omega t)+\frac{1}{2x^2}-\varepsilon_2 x\cos\omega t \tag{4.11}$$

with only square-root singularities, whose integrability properties can be detected using the methods described in this paper. First of all, it is important to note that the equation of motion associated with (4.11)

$$\ddot{x}=-x(1+\varepsilon_1\cos\omega t)+\frac{1}{x^3}+\varepsilon_2\cos\omega t \tag{4.12}$$

can be exactly solved for $\varepsilon_1=\varepsilon_2=0$ *to yield*

$$x_0(t)=[E+(E^2-1)^{1/2}\sin 2(t-t_0)]^{1/2} \tag{4.13}$$

where the two free constants are t_0 and E, the value of the Hamiltonian, or energy integral of the problem. The singularities of these solutions occur at $x_0(t_*^{(k)})=0$, i.e. at all $t=t_*^{(k)}$ where

$$E+(E^2-1)^{1/2}\sin[2(t_*^{(k)}-t_0)]=0. \tag{4.14}$$

This gives an infinite row of complex conjugate pairs, $t_*^{(k)}$, $\bar{t}_*^{(k)}$ located at a distance π from each other along the Re t axis.

Just as in the case of (4.1) with $\varepsilon=\delta=0$, cf. (4.2), the solution (4.13) is *globally* finitely sheeted and possesses, near its singularities, an expansion of the (4.4) type. However, when $\varepsilon_1\neq 0$ and/or $\varepsilon_2\neq 0$, all powers of $\tau^{1/2}$ enter in these expansions and the solutions are expressed by series of the form (4.10).

Now, as the ε_1 and ε_2 time-dependent terms are allowed to drive the motion and the Hamiltonian ceases to be a conserved quantity, one expects that the system will become non-integrable and chaotic orbits will be observed on a surface of section

$$\Sigma^{t_0}=\left\{x(t_k),\ \dot{x}(t_k),\ t_k=k\frac{2\pi}{\omega}+t_0,\ k\in\mathbb{Z}\right\} \tag{4.15}$$

$t_0\in\mathbb{R}$. However, when (4.12) was integrated in real time, with $\varepsilon_2\neq 0$ (and $\varepsilon_1=0$) and several initial conditions $x(t_0)$, $\dot{x}(t_0)$, *no* large-scale chaotic region was observed at first, even at ε_2 values as large as $\varepsilon_2=4.0$.

Another surprise was in store for us, when we put $\varepsilon_2=0$ and took $\varepsilon_1\neq 0$ in (4.11): Regular orbits were seen to exist *everywhere* on (4.15) and no chaotic behaviour was found, no matter how large the value of ε_1 we tried! So, what is going on here? Can the Hamiltonian (4.11) be integrable for all ε_1 and ε_2?

The answer to this question is suggested, by singularity analysis, in the following way: integrating the equation of motion (4.11) around one conjugate pair of singularities one always finds FSS, as in our earlier investigations of Hamiltonian systems [11, 12]. However, when integrating around two singularity pairs, very different results are obtained for the cases $\varepsilon_2=0$ and $\varepsilon_2\neq 0$:

The case $\varepsilon_2=0$ is characterized by FSS for all ε_1, exhibiting only the original four singularities of the primary sheet and returning to the starting values of the solutions, at some point P on the contour, after only a finite number of turns. On the other hand, if $\varepsilon_2\neq 0$, a very complicated pattern of singularities emerges within the contour and the differences of the solutions from their starting values at P after N turns, $\Delta x_P(N)$, oscillate chaotically away from zero, showing clear evidence of ISS, similar to what is depicted in figure 8(*b*).

These results suggest that the $\varepsilon_2=0$ case of (4.11) is integrable, whereas the $\varepsilon_2\neq 0$ is not. Returning then to our computations of orbits in real time, we discovered that for ε_2 big enough ($\varepsilon_2\geqslant 4.0$) large-scale chaos does eventually occur on the surface of section (4.15), demonstrating that the system is non-integrable in that case.

And what about the $\varepsilon_2=0$ case, which, according to our singularity analysis, should be integrable? Remarkably enough, this system does indeed possess an integral of the motion, which is an analytic single-valued function of x, $\dot{x}$ and t:

$$I=\tfrac{1}{2}(\rho\dot{x}-\dot{\rho}x)^2+\frac{\rho^2}{2x^3}=\text{constant}$$

$\rho(t)$ being a solution of Mathieu's equation, $\ddot{\rho}+(1+\varepsilon_1\cos\omega t)\rho=0$, as discovered by Lewis and Leach [24], in their investigations of integrable time-dependent Hamiltonian systems.

5. Discussion and concluding remarks

Undoubtedly, the distinction between integrability and non-integrability of dynamical systems has received and will continue to receive a lot of attention in the scientific literature. Although it is very often related to the possible existence of chaos in a physical system, it remains primarily a mathematical question since, as is well known, there are many *non-integrable* systems, whose orbits are perfectly regular and exhibit

no chaotic behaviour anywhere in their phase space (e.g. in the presence of a globally attracting fixed point!).

Now, there exists, to date, a considerable amount of literature which suggests that the integrability of a dynamical system is closely connected to the mathematical simplicity of its solutions as functions of time and initial conditions. But what does mathematical simplicity mean in this context and how can it be quantified?

The singularity analysis of the solutions of a dynamical system in *complex time* offers a possible answer to this question: essentially, the main idea is that simple functions are those which are single-valued (except for isolated poles), or have a globally finite sheeted structure, whereas complicated functions are infinitely sheeted with a complicated pattern of singularities in the complex t-plane.

Rigorous results on the question of integrability have been proved so far in two cases: when the solutions have only poles (the Painlevé property) and when they have infinitely branched singularities, i.e. contain terms of the form $(t-t_*)^{\lambda}$, with λ irrational or complex, in their series expansions near a singularity $t=t_*$ [1–8].

In this paper, we continued our investigation of the intermediate case of algebraic singularities [11, 12], in which the solutions of a dynamical system contain only powers of $(t-t_*)^{p/q}$ (p/q=rational) and hence are *locally* finitely branched and finitely sheeted. In particular, we considered several examples of physical interest, with only square-root singularities (i.e. powers of $(t-t_*)^{1/2}$ in their series expansions) and studied numerically their analytic structure in integrable and non-integrable cases.

Our main result, in agreement with earlier studies, is that it is possible for such systems to exhibit *infinitely sheeted solutions* (the ISS property) when integrated along large enough contours containing a sufficient number of singularities. The main equation studied in this paper describes a three-parameter family of Duffing–van der Pol oscillators (DVP), equation (1.1).

One starts by integrating numerically in the complex t-plane around closed contours, which enclose at least one singularity of the primary sheet of the solution, near $t=0$. If the contour is relatively short, only a small number of singularities will be observed, arising on different sheets and the solution will return to its original value, at some point P of the contour, after a finite number of turns (FSS=finite sheeted solutions). However, as the contour is increased beyond a certain critical size, which encompasses one crucial singularity of the solution, a dramatic change occurs: new singularities keep appearing, at every turn, whose branching does not allow the solution to return to its original value, thus providing strong evidence of ISS.

If the system is integrable, however, no such change occurs. The solutions are always seen to return, exactly, within the accuracy of our computations (10^{-11}–10^{-14}), to their initial values no matter how large the contour and how many singularities are enclosed within it.

Thus, we propose that the ISS property is a *necessary* condition for *non-integrability*. We also suggest that looking for ISS or FSS in complex time, may be a useful method for identifying integrable cases, in multi-dimensional or other systems, which are too difficult or too costly to analyse by real-time techniques. In many cases, we have also found that certain ISS phenomena (like the density of singularity patterns or the magnitude of the differences of the solutions from their initial values) increase significantly as a nonlinearity or forcing parameter is increased and the motion becomes more chaotic in real time.

Clearly, our approach so far has been primarily numerical. This is partly justified by the fact that our investigations concern *global* properties of solutions which are very

difficult to determine by analytical techniques. Further work is needed, of course, to rigorously validate our findings.

We believe that such work is worth pursuing, as it is expected to enable us to improve our understanding of (non-)integrability and find new relationships between the real time motion of a dynamical system and the mathematical properties of its solutions in complex time.

Acknowledgments

One of the authors (TB) would like to thank the Center of Nonlinear Dynamics of Bharathidasan University, Tiruchirapalli, India University for its kind hospitality, during his stay there, where part of the work reported in this paper was completed.

References

[1] Ziglin S L 1983 *Funct. Anal. Appl.* **16** 181; *Funct. Anal. Appl.* **17** 6
[2] Ziglin S L 1982 *Trans. Moscow Math. Soc.* **1** 283
[3] Yoshida H 1983 *Celestial Mech.* **31** 363, 381
[4] Yoshida H 1987 *Physica* **29D** 128; 1989 *Phys. Lett.* **141A** 108
[5] Bountis T 1992 *Int. J. Bif. Chaos* **2** 217
[6] Chang Y F, Tabor M, Weiss J 1982 *J. Math. Phys.* **23** 531; 1983 *Physica* **8D** 380
[7] Bountis T, Papageorgiou V and Bier M 1987 *Physica* **24D** 292
[8] Ramani A, Grammaticos B and Bountis T 1989 *Phys. Rep.* **180** 160
[9] Hietarinta J, Grammaticos B, Dorizzi B and Ramani A 1984 *Phys. Rev. Lett.* **53** 1707
[10] Goriely A 1992 *Chaotic Dynamics: Theory and Practice* ed T Bountis (London: Plenum)
[11] Bountis T C, Drossos L B and Percival I C 1991 *Phys. Lett.* **159A** 1
[12] Bountis T C, Drossos L B and Percival I C 1991 *J. Phys. A: Math. Gen.* **24** 3217
[13] Okuda M 1981 *Progr. Theor. Phys.* **66** 90
[14] Rajasekar S and Lakshmanan M 1988 *Physica* **32D** 146
[15] Rajasekar S, Parthasarathy S and Lakshmanan M 1992 *Chaos, Solitons and Fractals* **2** 271
Rajasekar S and Lakshmanan M 1992 *Int. J. Bif. Chaos* **2** 201; 1993 *Physica* **D** (to appear)
[16] Dimitriev A S, Komlev V A and Turaev D 1992 *Int. J. Bif. Chaos* **2** 93
[17] Parthasarathy S 1990 *Symmetries and Singularity Structures* ed M Lakshmanan and M Daniel (Berlin: Springer)
[18] Parthasarathy S and Lakshmanan M 1990 *J. Phys. A: Math. Gen.* **23** L1223; 1991, *Phys. Lett.* **157A** 365
[19] Drossos L B and Bountis T C 1992 *Chaotic Dynamics: Theory and Practice* ed T Bountis (London: Plenum)
[20] Chang Y F and Corliss G 1980 *J. Inst. Math. Appl.* **25** 349
[21] Nayfeh A and Mook T 1979 *Nonlinear Oscillations* (New York: Wiley)
[22] Bountis T C, Bier M and Papageorgiou V 1990 *Symmetries and Singularity Structures* ed M Lakshmanan and M Daniel (Berlin: Springer)
[23] Fournier J D, Levine G and Tabor M 1988 *J. Phys. A: Math. Gen.* **21** 33
[24] Lewis H R And Leach P G L 1982 *J. Math. Phys.* **23** 2371